Effect of tree roots on a shear zone: modeling reinforced shear stress

KAZUTOKI ABE
Forestry and Forest Products Research Institute, Tsukuba, Ibaraki 305, Japan
AND
ROBERT R. ZIEMER
USDA Pacific Southwest Research Station, Forest Service, Arcata, CA 95521, U.S.A.

Received September 10, 1990
Accepted January 30, 1991

ABE, K., and ZIEMER, R. R. 1991. Effect of tree roots on a shear zone: modeling reinforced shear stress. Can. J. For. Res. **21:** 1012-1019.

Tree roots provide important soil reinforcement that improves the stability of hillslopes. After trees are cut and roots begin to decay, the frequency of slope failures can increase. To more fully understand the mechanics of how tree roots reinforce soil, fine sandy soil containing pine roots was placed in a large shear box in horizontal layers and sheared across a vertical plane. The shapes of the deformed roots in the sheared soil were explained satisfactorily by an equation that had been developed to model the deformed shape of artificial reinforcement elements, such as wood dowels, parachute cord, Bungy cord, and aluminum rods. Root deformation in sheared soil is influenced by the diameter and concentration of roots. A model is proposed that uses root strain to estimate the shear stress of soil reinforced by roots. The shear resistance measured from the shear tests compared quite well with the model simulation.

ABE, K., et ZIEMER, R. R. 1991. Effect of tree roots on a shear zone: modeling reinforced shear stress. Can. J. For. Res. 21 : 1012-1019.

Les racines des arbres constituent un élément important de renforcement du sof qui augmente la stabilité des pentes. Lorsque les arbres sont coupes, les racines se décomposent et la fréquence des glissements de terrain a tendance à augmenter. Dans le but de mieux comprendre le mécanisme par lequel Ies racines des arbres renforce le sol, un sol composé de sable fin contenant des racines de pin a été placé en couches horizontales dans de larges boîtes et soumis au cisaillement le long d'un plan vertical. La deformation des racines soumises au cisaillement dans le sol pouvait être expliquée de façon satisfaisante par une equation développée pour modéliser la deformation d'éléments artificiels de renforcement tels que des chevilles de bois, de la corde de parachute, de la corde à bondonner et des tiges d'aluminium. La 'deformation des racines soumises au cisaillement dans le sol est fonction du diamètre et de la concentration des racines. Un modèle utilisant la résistance des racines est propose pour estimer l'effort de cisaillement que peut supporter un sol renforcé par des racines. La résistance au cisaillement mesurée par des tests Concorde avec la simulation fournie par le modèle.

[Traduit par la redaction]

Introduction

Several approaches have been used to describe the function of forests in preventing landslides. For example, statistical studies have correlated landslide frequency with forest condition (Namba et al. 1975). Other studies have analyzed slope stability using root tensile strength (Burroughs and Thomas 1977; Ziemer and Swanston 1977) or the force required to pull roots from the soil (Tsukamoto 1987). And still other studies have evaluated the shear strength of rooted soil.

To predict and prevent the sediment problems that follow changes of vegetation due to forest management and development in mountain areas, it is important to fully understand the mechanics of how roots reinforce soil. Waldron (1977) and Wu (1976) presented similar models that describe the shear strength of rooted soil:

$$[1] \quad Sr = c + \sigma \tan \phi + AS$$

where

- Sr is the shear resistance of rooted soil
- ΔS is the contribution of roots to soil shear resistance
- c is the soil cohesion
- σ is the normal stress
- ϕ is the angle of internal friction of the soil

$$[2] \quad AS = a_r \, Tn(\sin \beta + \cos \beta \tan \phi)$$
$$Tn = (4\tau' EZ/D)^{1/2}$$

where

- Tn is the maximum tensile stress in the root
- a_r is the cross-sectional area of the root
- τ' is the maximum tangential friction between root and soil
- E is Young's modulus (which is the stretch modulus; i.e., the ratio between normal stress and elastic strain)
- Z is the shear zone width
- D is the diameter of the root
- β is the angle of root deformation

In their model, a horizontal element of the tensile stress directly enhances the shear stress, and a vertical element contributes to the normal stress (Fig. 1). Using results from direct shear tests, Gray and Ohashi (1983) modified this model to account for the initial orientation of the fibers. Waldron and Dakessian (1981) also altered the model to include the effects of root stretching, slipping, and breaking. They also simulated the influence of changing the thickness of the shear zone. Shewbridge and Sitar (1985) pointed out that the thickness of the shear zone and the deformed shape of the roots significantly influence reinforced shear strength (ΔS). They investigated such influences by using wood dowels, parachute cord, Bungy cord, and aluminum rods. Shewbridge and Sitar (1985) developed eq. 3 to model the shape of the deformed reinforcement elements and reported that the thickness of the shear zone

Printed in Canada / Imprimé au Canada

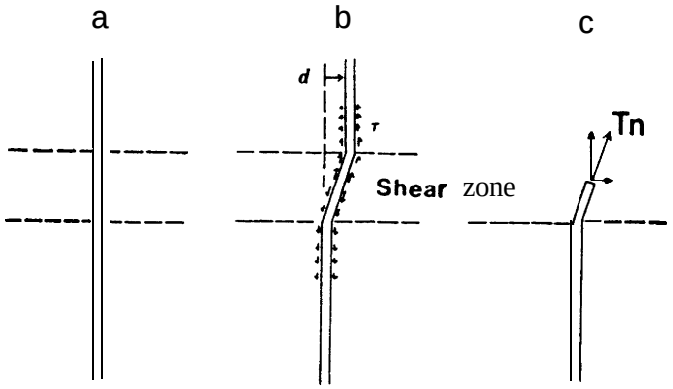

FIG. 1. Root reinforcement model by Waldron (1977). Flexible, elastic root extends vertically across a horizontal shear zone. (*a*) Undisturbed soil. (*b*) Upper mass of soil displaced, *d*. Tangential friction, τ, is generated with extension of the root. (*c*) Horizontal and vertical factor of maximum tensile stress, Tn, in the root reinforces the shear resistance of rooted soil.

TABLE 1. Summary of the number of roots and their individual diameters used in each test

Test No.	No. of roots	Roots used in test	Symbol of root	Mean diam., *D* (mm)
1	0	—	*a*	8.18
2	0	—	*b*	7.91
3	3	*a,b,c*	*c*	8.19
4	3	*a,b,c*	*d*	13.69
5	3	*d,e,f*	*e*	12.97
6	3	*d,e,f*	*f*	11.06
7	9	*a,b,c,d,e,f,g,h,i*	*g*	8.69
8	6	*a,c,d,f,g,i*	*h*	9.96
9	6	*a,c,d,f,g,i*	*i*	9.76
10	9	*a,b,c,d,e,f,g,h,i*		
11	0	—		

agrees with the range of the calculated deformation. The coordinate (x, y) shows the deformed shape:

$$[3] \quad y = B - B\, e^{-b|x|}$$

where

y is the axis parallel to the direction of shear
x is the axis perpendicular to the direction of shear
B is one-half the distance between asymptotes (which is one-half of shear displacement)
b is a parameter modified to improve the fit

Shewbridge and Sitar (1985) further developed a work model based on eq. 3.

To further investigate the shape of deformed roots after shear, we made large-scale direct shear tests. From these data, a modified AS model was developed.

Shear device

A large shear device (Fig. 2) was used to perform the tests. The shear box has two halves, a stationary half and a sliding half. The soil and roots were placed into the shear box in horizontal layers and sheared across a vertical plane between the two halves. The sliding half is capable of a maximum of 100 mm of total displacement. The shear force was provided by a hand-operated screw jack and measured using a double proving ring. The deformation of the roots and

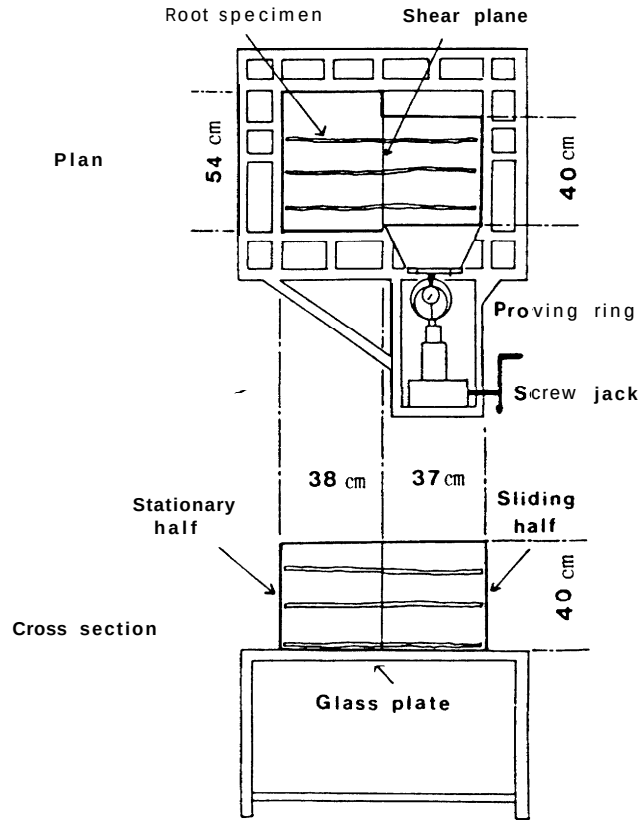

FIG. 2. Direct shear device. Shear plane is formed on a vertical interface between stationary and sliding halves of the shear box. Roots are set horizontally, perpendicular to the shear plane, and in three layers to distribute root effects evenly within the fine sand.

the development of the shear zone were observable through a double-glass bottom of the shear box.

Fine sand with a dry density of 1.47 g·cm^{-3} and a moisture content of 19.5% by weight was used in the experiments. For each test, a total of 90.5 kg of sand was placed and compacted in the shear box in five 18.1-kg layers, Finally, 250 kg of lead shot was placed on top of the sand to keep the overburden stress distribution uniform throughout the test. The normal stress on the bottom glass was 0.0964 kg·cm^{-2}.

The roots used for the test were collected from shore pine *(Pinus contorta* Dougl. var. *contorta),* a species that is commonly found growing along the west coast of North America. Only straight roots without branches, bends, or visible defects were selected. The number of roots used in each test and their average diameters are summarized in Table 1. The roots were placed in the shear box in three vertical layers to obtain a uniform distribution of the ΔS effect in the sand. For example, in a three-root test, one root was set in each layer: one root near the bottom adjacent to the glass plate, one about 5 cm above the bottom, and one about 10 cm above the bottom (Fig. 2). To observe the development of the shear zone, 1cm wide belts of white sand were placed on the bottom glass and oriented perpendicular to the direction of shear. Before and after the tests, the shape of the roots and the white sand belts were mapped.

A screw jack was used to shear the root-sand composite and to make a total displacement of 88 mm at a constant rate for 7 mm. The dial gage of the proving ring was read

TABLE 2. Characteristics of deformation of roots on the shear-box glass and its relationship to coefficient of deformation, *b*, obtained from eq. 4

Test No.	No. of roots	Roots area ratio, A_r/A (%)	Roots on glass No.	Roots on glass Symbol	Mean diam., D (mm)	Coeff. b (cm^{-1})	r^2 (%)
1	0						
2	0						
3	3	0.2573	1	*a*	8.18	0.197	96.5
4	3	0.2573	1	*d*	8.18	0.201	86.8
5	3	0.6225	1		13.69	0.160	96.2
6	3	0.6225	1	*f*	11.06	0.163	60.0
7	9	1.2315	3	*g*	8.69	0.126	92.1
				h	9.96	0.129	88.5
				i	9.76	0.116	97.0
8	6	0.8017	2	*a*	8.18	0.171	95.5
				c	8.19	0.140	96.3
9	6	0.8017	2	a	8.18	0.171	95.5
				c	8.19	0.140	96.3
10	9	1.2315	3	*d*	13.69	0.114	96.8
				e	12.97	0.108	95.1
				f	11.06	0.141	91.4
11	0						

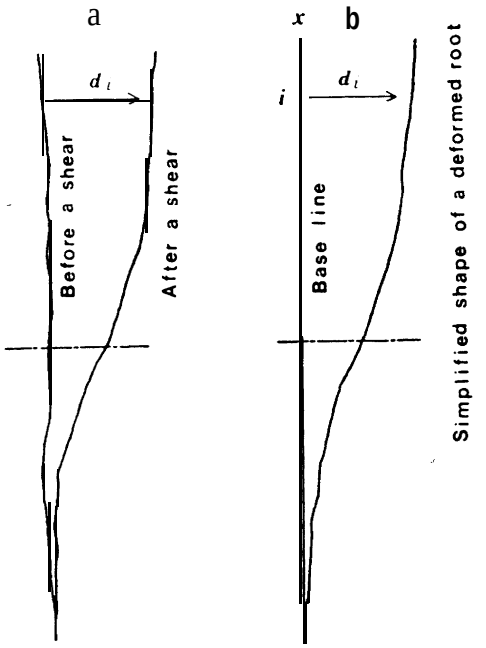

FIG. 3. Map of roots before and after deformation. (*a*) Original root shape before and after a shear test. (*b*) Displacement, d_i, at $x = i$ is remapped from a straight base line to simplify root deformation.

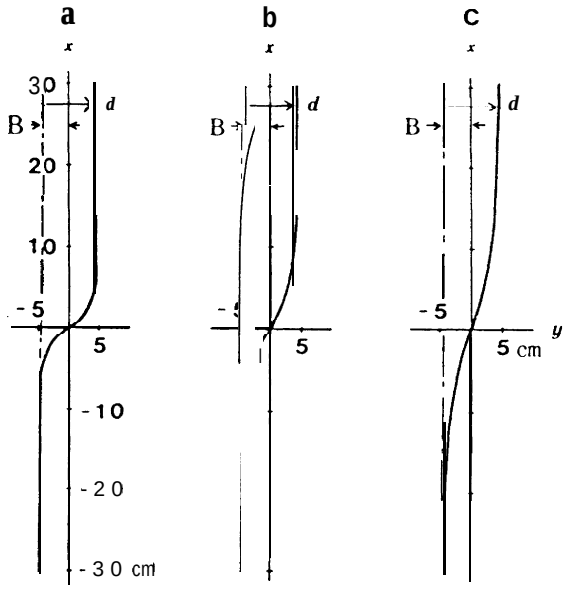

FIG. 4. Differences in deformed shape influenced by coefficient *b*. (*a*) Bungy cord (b = 0.5 cm^{-1}). (6) Root *a* (*b* = 0.197 cm^{-1}). (*c*) Root *i* (*b* = 0.116 cm^{-1}). These were mapped using eq. 3 after 88 mm displacement (B = 44 mm).

every 5 s until the end of each test. Changes in the position of the roots and white belts were videotaped through the bottom glass as the test proceeded.

Test results

Root deformaion

The shape of each root near the glass plate, including natural bends, was mapped before and after the test (Fig. 3*a*). Then, the difference in position of the root before and after the shear was measured at l-cm intervals along the *x*-axis; d_i, and remapped as displacement from a straight base line (Fig. 3b).

The complex shape of the root was simplified to a smoothed curve for mathematical modeling. These smoothed shapes of the deformed roots were compared with estimates using eq. 3, which was developed by Shewbridge and Sitar (1985), using artificial surrogates for woody roots. This model of deformation does not agree with Waldron's (1977) model, where the root abruptly bends at boundaries between the shear zone and outer undisturbed zone. We observed that the root deformed in a wider range than the shear zone and had smooth, not abrupt, bends.

The modeled root deformation shape depends on the coefficient of deformation, *b*, in eq. 3. A large value of *b* corresponds to a reinforcement element with little stiffness and results in an abrupt deformation near the shear zone. For

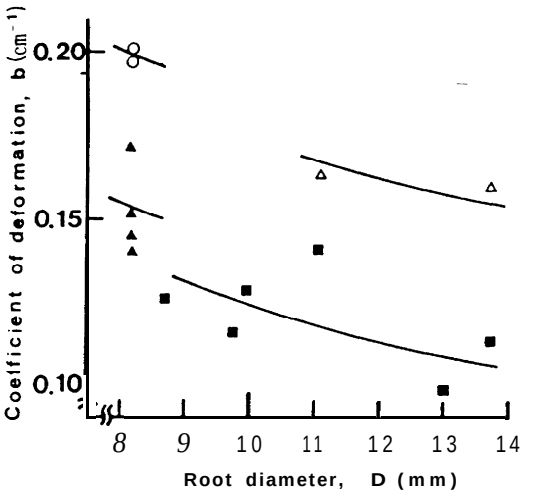

FIG. 5. Influence of diameter and root area ratio (A_r/A) on coefficient *b*. o, A_r/A = 0.26%; A, 0.62%; A, 0.80%; ● , 1.23%. A multiple regression equation [4] is obtained.

TABLE 3. Width of shear zone in each test

Test No.	No. of roots	Shear zone Z_2 (cm)			Shear zone Z_3 (cm)		
		Right	Left	Mean	Right	Left	Mean
1	0						
2	0						
3	3	5.7	5.0	**5.4**	***18.0***	13.0	15.5
4	3	**4.8**	**5.8**	**5.3**	**14.0**	**15.0**	**14.5**
5	3	**4.0**	**4.4**	**4.2**	**21.0**	16.0	**18.5**
6	3	**6.1**	**6.4**	**4.3**	20.0	24.0	22.0
7	9	10.0	14.6	12.4	31.0	35.0	33.0
8	6	7.0	6.3	6.7	26.0	31.0	28.5
9	6	9.3	–*	**10.2**†	30.0	28.0	29.0
10	9	–*	10.6	**10.6**†	34.0	37.0	35.5
11	0	4.5	1.8	3.2	8.0	8.0	8.0

NOTE: The white sand bands were not set in tests 1 and 2.
● Z_2 is not clear.
†Values were assumed by observation of the shear zone.

example, a Bungy cord has a *b* of about 0.5 cm^{-1} (Fig. *4a)*. As the reinforcement element increases in stiffness, the value of *b* decreases and the curvature becomes more gentle and extends over a greater length (Figs. *4b* and *4c*). The roots we used had a coefficient *b* that ranged from about 0.1 to 0.2 cm^{-1} (Table 2). The shape of the root deformation agreed well with that produced using eq. 3. The explained variance (r^2) between observed and modeled shape of the roots ranged from 0.60 to 0.97 (Table 2), with an average of 0.91.The value of *b* seemed to be affected by the root diameter and the concentration of roots, expressed as root area ratio (A_r/A) (Fig. 5). In general, large values of *b* corresponded to small values of A_r/A and small roots, indicating a more narrow deformation zone. The following multiple regression was developed for *b* from the data (Table 2):

$$[4] \quad b = 0.2262 - 0.0715\ (A_r/A) - 0.0016D \qquad r^2 = 0.88$$

where

b is the deformation modulus (cm^{-1})
D is the diameter of the root (mm)

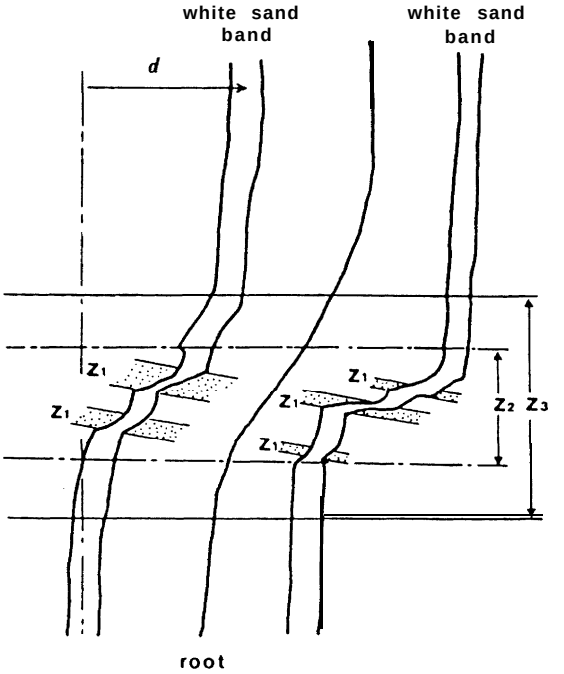

FIG. 6. Mapped shear zone and deformed root in test 3. Deformation of white sand bands shows three sheared zones (Z_1, Z_2, and Z_3) that have different strain.

A_r is the total root area in the shear plane (mm^2)
A is the area of the shear plane (mm^2)

Development of sand shear zone

Roots in sheared sand affect the development of the sand shear zone by relative movement among sand particles. This could clearly be seen by observing the changes of the white sand belt on the bottom glass of the shear box (Fig. *6*). The amount of sand strain was not uniform within the shear zone. The largest strain, Z_1, was produced in the middle of the shear zone. For shear tests without roots, the width of Z_1 often approached a narrow line. The orientation of Z_1 was formed at a slight angle to the horizontal plane. Zone Z_2 included Z_1, and the average strain in Z_2 was less than in Z_1. Zone Z_3 was located at the outer sides of Z_2. Here, the white band curved slightly and smoothly, but Z_1, was never found within Z_3

The width of the shear zone was increased by the presence of roots in shearing sand (Table 3). In tests with no roots, Z_1 was often nearly a line and most of the strain was concentrated along Z_1 and the shear zone Z_3 was very narrow (about 8 cm).

In contrast, the width of Z_3 in tests using nine roots extended more than 30 cm, but Z_1 never developed. In the tests, deformation of the white bands was constant and smooth, making gentle curves throughout the range of Z_3. Their shape tended to look like that of the deformed roots. For the tests using three and six roots, the width of Z_3 was intermediate between tests with no roots and those with nine roots.

Zone Z_1 became more indistinct with increasing concentration of roots. This implies the decentralization shear strain. Palmeira and Milligan (1989) showed that a significant reduction in shear strain developed along the central region of a shear box by reinforcements in their large-scale direct shear tests. The range of root deformation is not equal

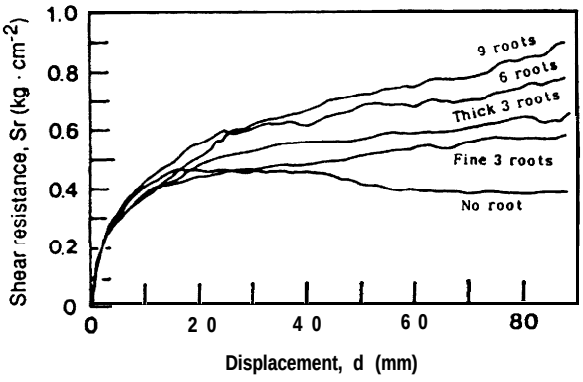

FIG. 7. Shear resistance, Sr, increases with increasing root concentration.

to the sand shear zone. The observed sand shear zone formed inside the root deformation zone, but the sand particles extremely close to the roots seemed to move the same as the roots.

Reinforced shear resistance, AS

In shear tests with no roots, the maximum shear resistance occurred at 17 mm of displacement, after which resistance gradually decreased to a residual strength at a displacement of 70 mm (Fig. 7). For all of the tests that contained roots, shear resistance, Sr, continually rose and the upper yield point was not reached even at 88 mm of displacement. Shear resistance increased both with increasing displacement and with increasing number of roots.

Discussion

Modification of the AS *model*

When a root in shearing sand deforms (Fig. 8), it is elongated by a displacement, *d*. The strain on the root that is generated by this elongation produces a tensile stress:

[5] $T = E\,\varepsilon$

where

T is the tensile stress in the root
E is Young's modulus
ε is the strain in the root

The maximum shear strength occurs at the point 0 (Fig. 8), where the moment is zero. It equilibrates to the total earth pressure acting on the root and can be expressed by eq. 6:

[6] $\Delta S_p = D \int_0^{M'} p\,dx$

where

ΔS_p is the shear length applied to a root by earth pressure
D is the diameter of root
P is the earth pressure
M' is the top point of deformation

Thus, two factors contribute to soil reinforcement, as shown in eq. 7:

[7] $AS = AS_t + \Delta S_p$

where ΔS_t is the reinforced strength caused by tensile stress of a root.

Effect of tensile stress

Tree root deformation can be expressed by eq. 3 as discussed earlier. As the deformation is symmetric with respect

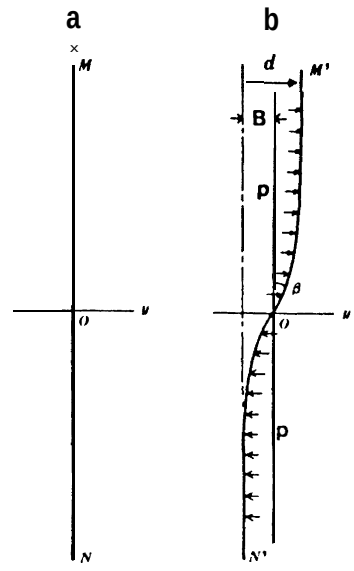

FIG. 8. Model illustration. (*a*) Intact root. (*b*) Deformed root after it is displaced, *d*, makes an angle, β, at the origin, 0, and earth pressure, *p*, is generated.

to the origin, the shape of the deformed root can be evaluated using only one side of the *x*-axis. Thus, a length of deformed root can be calculated as

$$dl^2 = dx^2 + dy^2$$

and

[8] $l = 2\int_0^{M'} (1 + B^2b^2\,e^{-2bx})^{1/2}\,dx$

where

l is a length of deformed root
B is one-half of a shear displacement
b is a parameter modified to improve the fit
dl is a root length in an infinitely short section dx after shear
dx is an infinitely short interval of *x*-axis
dy is an infinitely short interval of *y*-axis

By differentiating eq. 8, an elongated ratio, *V*, is obtained. It is a dependent variable of *x* and can be expressed as in eq. 9:

[9] $V(x) = dl/dl_0 = (1 + B^2b^2\,e^{-2bx})^{1/2}$

where

$V(x)$ is an elongated ratio of the root
dl_0 is a length of the root in an infinitely short section

Strain in the root is shown by eq. 10:

[10] $\varepsilon = dl'/dl_0 = dl_0\{V(x) - 1\}/dl_0 = V(x) - 1$

where

ε is the strain in the root
dl' is an elongated length in an infinitely short section after shear

Substituting eq. 9 into eq. 10

[11] $\varepsilon = (1 + B^2b^2\,e^{-2bx})^{1/2} - 1$

ε shows the maximum at $x = 0$, so the maximum tensile stress is given by substituting eq. 10 into eq. 5:

[12] $Tn = \{V(0) - 1\}E$

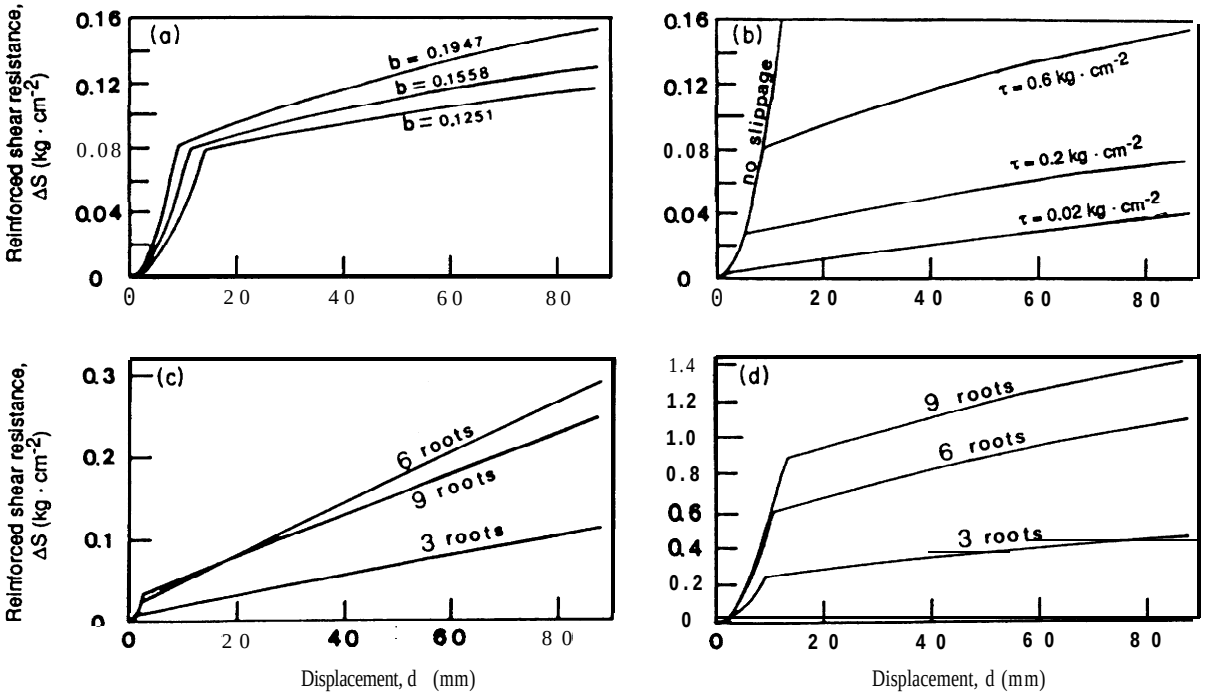

FIG. 9. Estimation of coefficient of deformation, b, tangential friction, τ, and root concentration by the model simulation as they affect AS. (*a*) Effect of coefficient of deformation, b, on ΔS. AS of root *a* was calculated using the values 0.1947, 0.1558, and 0.1251 cm^{-1} for b obtained from eq. 4, as the simulation value of the three-, six-, and nine-roots test, respectively, and using a constant τ of 0.6 $kg \cdot cm^{-2}$. (*b*) Effect of tangential friction, τ, on AS. AS of root *a* was calculated with τ of 0.02, 0.2, 0.6 kg-cm^{-2}, and no slippage using a constant b of 0.1947 cm^{-1}, (*c*) Effect of root concentration on ΔS. AS was calculated for three, six, and nine roots using a constant τ of 0.02 $kg \cdot cm^{-2}$. (*d*) Effect of root concentration on AS. AS was calculated for three, six, and nine roots using a constant τ of 0.6 kg cm^{-2}.

where Tn is the maximum tensile stress in the root. Then, the effect of stretching on the reinforced strength is shown in eq. 13 by substituting eqs. 11 and 12 into eq. 2.

$$[13]\quad \Delta S = \{[(1 + B^2b^2\, e^{-2bx})^{1/2} - 1]Ea_r\} \times (\cos\beta \tan\phi + \sin\beta)$$

where β is an angle made by the x-axis and the root, obtained as follows:

$$[14]\quad (dy/dx)_{x=0} = bB$$

$$\beta = \tan^{-1}(bB)$$

On the other hand, AS, is obtained by a deflection equation:

$$[15]\quad \Delta S_p = EI(d^3y/dx^3)_{x=0}$$

where

E is Young's modulus (stretch modulus)
I is the modulus of the section

Substituting eq. 3 into eq. 15

$$[16]\quad \Delta S_p = EIb^3B$$

Finally, AS is shown by

$$[17]\quad \Delta S = \{[(1 + B^2b^2\, e^{-2bx})^{1/2} - 1]Ea_r\} \times (\cos\beta \tan\phi + \sin\beta) + EIb^3B$$

Slippage and breakage of the roots

The soil causes root tension by tangential stress, τ, at the soil and root interface, and this stress has a maximum value of τ' at incipient slippage. Equation 18 shows the maximum tension, Tn_s, just before the incipient slippage (Waldron and Dakessian 1981):

$$[18]\quad Tn_s = 2\tau'(t/D)$$

where

τ' is the maximum stress of tangential friction
L is the length of the root
D is the diameter of the root

When the tension in the root exceeds the rupture stress of the root, Tn_f, the root will break. This can be expressed by eq. 19:

$$[19]\quad Tn_f = 2\tau' l_f/D$$

where

τ' is the maximum stress of tangential friction
l_r is the length of root required for producing Tn_f
D is the diameter of the root

Accordingly, the root will be broken under the following condition:

$$\{(1 + B^2b^2)^{1/2} - 1\}E > Tn_s \text{ and } L > l_f$$

and it will slip when

$$\{(1 + B^2b^2)^{1/2} - 1\}E > Tn_s \text{ and } L < l_f$$

Model simulation

To calculate ΔS, the coefficients in the model were determined as follows. The value for Young's modulus, E, was determined to be 27.6 x 10^3 $kg \cdot cm^{-2}$ by preliminary root tension tests conducted with *Cryptomeria japonica* D. Don (Abe and Iwamoto 1986). We assumed that this value was

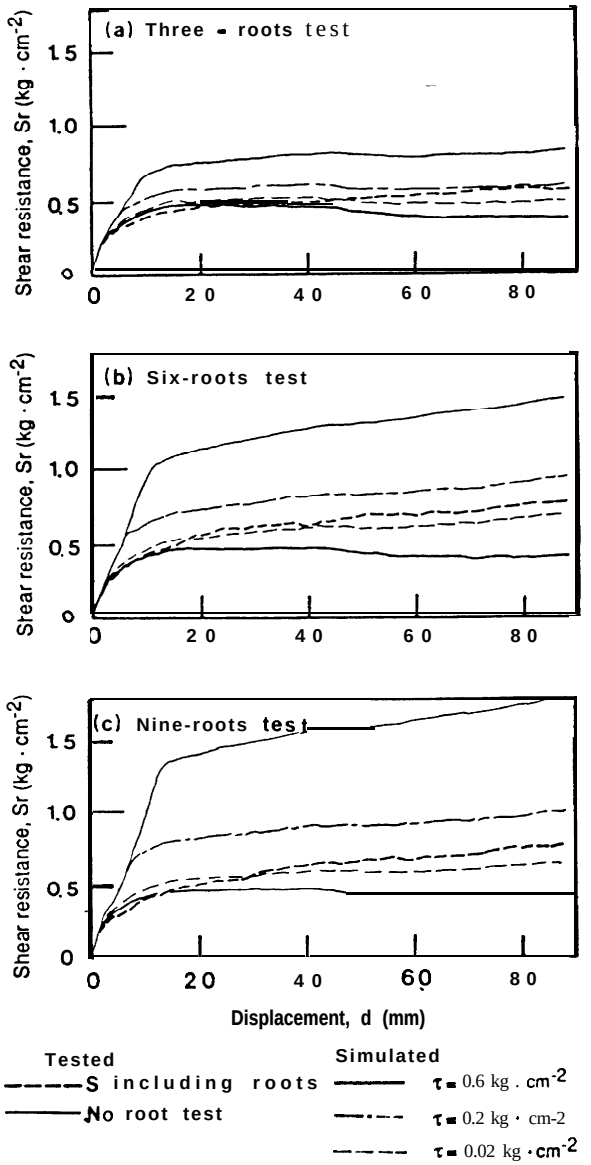

FIG. 10. Comparison between tested and simulated shear resistance of the (*a*) three-roots, (*b*) six-roots, and (*c*) nine-roots test. Values of τ of 0.02, 0.2, and 0.6 kg· cm^{-2} were used in each simulation.

the same for shore pine and *C. japonica*. The value for ϕ was assumed to be 35. Values for τ' of 0.02, 0.2, and 0.6 kg·cm^{-2} were applied in the model. Length of the root was measured to be 72 cm.

Effect of coefficient of deformation, b, *on* AS

Root *a* was used in tests having three, six, and nine roots. The values of *b* calculated by eq. 4 were 0.1947, 0.1558, and 0.1251 cm^{-1}, respectively. The values of a_r/A and *D* shown in Table 2 were used in this calculation to have the same conditions for the simulation as was measured in the tests. Smaller values of *b* indicate a more gentle curve of the deformed root (Fig. 4). As the value of *b* increases, the root deforms more, and A*S* increases as the root stretches (Fig. *9a)*. The point of incipient slippage occurs at shorter displacements as the value of *b* increases. For example, incipient slippage occurs at about 9 mm when *b* is 0.1947 cm^{-2}, and at 14 mm when *b* is 0.1251 cm^{-1}. After incipient slippage, the value of AS increases at a higher rate for greater values of *b*. In other words, as roots become more deformed, they tend to produce greater reinforced strength.

Effect of tangential friction, τ, *on* AS

Values for AS were calculated for roots having values of tangential friction, τ, of 0.02, 0.2, and 0.6 kg cm^{-2}, while the value of *b* was held constant at 0.1947 cm^{-1} (Fig. *9b)*. So long as τ is strong enough to prevent slippage, the stretched root makes a rapid contribution to A*S*. Once the root begins to slip, the rate of contribution to A*S* is reduced.

When τ is 0.02 kg·cm^{-2}, the contribution of root stretching to A*S* is almost not generated. There have been virtually no investigations to determine the field value of τ for actual tree roots.

Effect of root concentration on AS

The most important influence of roots on the total reinforced shear resistance, A*S*, is the point at which the roots begin to slip, When tangential friction, τ, is high, AS increases substantially as the number of roots increases (Fig, *9d)*. Once slippage occurs, however, further increases in the maximum shear resistance, A*S*, is strongly influenced by the coefficient of deformation, *b*, expressed in the formula (EIb^3B) [16]. Because the average value of *b* per root becomes smaller **as** the concentration of roots in sand increases (Table 2), after slippage, the slope of the relationship between displacement and A*S* becomes smaller as the number of roots increases (Figs. *9c, 9d)*.

Simulation for the test results

Observed and simulated shear resistance, Sr, was compared for tests using three, six, and nine roots (Figs. *10a, 10b,10c)*. The values of tangential friction, τ, used in the simulations were 0.02, 0.2, and 0.6 kg ·cm^{-2}. Simulated Sr was calculated by adding A*S* obtained using the model to the shear resistance of the shear tests without roots. Observed Sr values of rooted soil tend to be lower than simulated Sr at the beginning of displacement.

This is because the model does not consider that a displacement is needed to extend a deflected root before it will be in tension, But, in general, simulated Sr with τ = 0.02 kg·cm^{-2} agrees with the observed Sr better than simulated Sr with other values of τ. It appears that the model is good enough to simulate Sr over the range of observed displacement.

Summary and conclusion

Direct shear tests were conducted on a fine sand reinforced with shore pine roots. Deformation of the roots was observed through a bottom glass of the shear apparatus. This deformation was expressed by eq. 3. A theoretical model of reinforced strength was modified to consider root deformation. Experimental shear resistance was compared with the model simulation. From this comparison, we conclude the following:

(1) The reinforced shear resistance, A*S*, increases rapidly by stretching before the roots slip. A*S* also increases gradually after the slippage, with the rate of increase related to the tangential friction between the root and soil, τ, and earth pressure generated on the roots.

(2) The amount of tangential friction, τ, is the most significant factor contributing to A*S*. The greater τ becomes,

the greater AS becomes, because the roots can stretch rather than slip. The value of τ in the tests was about 0.02 kg . cm $^{-2}$. Under actual field conditions, t should be much greater because of root hairs, bending, and branching of roots. However, to date, there has been little fieldwork to develop such values.

(3) The amount of root deformation increases as the number of roots and the size of the roots decrease in the shearing soil, so the reinforced strength provided by one root is more effective. When soil is loose, AS becomes less as the number of roots increases, because of a smaller root deformation in the shearing soil which includes more roots. For their experimental conditions, Gray and Ohashi (1983) indicated that deformation and stiffness of fiber (root) seem to be significant factors that provide reinforcement to the soil shear strength.

(4) The presence of roots causes a widening of the shear zone. With a wider shear zone, each soil particle is required to move less than when the shear zone is more narrow. Shewbridge and Sitar (1985) pointed out that the widening of the shear zone will result in a higher internal friction angle, ϕ, for the Mohr-Coulomb failure envelope after a given strain. Mogami and Imai (1969) conducted biaxial compression tests on a single layer of equal-sized steel balls. When an assemblage of balls undergoes shearing deformation, several densely packed parts appear, as well as several loosely packed parts. The larger the surface friction, the larger the influence zone. However, for most shear tests of rooted soil, increases in soil shear strength have traditionally been assigned to enhancing soil cohesion. In the model we have proposed, AS is added to the cohesion term in spite of the observed widening of the shear zone. There is need of more theoretical work related to shear zone widening and the AS model.

(5) The model simulation corresponded quite well with the shear tests.

Acknowledgement

This research was partially supported by a grant from the Science and Technology Agency of Japan.

ABE, K., and IWAMOTO, M. 1986. An evaluation of tree-root effect on slope stability by tree-root strength. J. Jpn. For. Soc. **68**: 505-510.

BURROUGHS, E.J., JR., and THOMAS, B.R. 1977. Declining root strength in Douglas-fir after felling as a factor in slope stability. USDA For. Serv. Res. Pap. INT-190.

GRAY, D.H., and OHASHI, H. 1983. Mechanics of fiber reinforcements in sand. J. Geotech. Eng. Div. **108**(GT3): 335-353.

MOGAMI, T., and IMAI. G. 1969. Influence of grain to grain friction on the shear phenomena of granular material. Soils Found. 9(3): l-15.

NAMBA, S,, AKIYA, K., YANASE, H., KONO, R., TAKESHITA, M., and SHIMIZU, T. 1975. Forest influence upon landslides occurred by heavy rainfall in June 1972. Science and Technology Agency, Tokyo. Special research report on sediment disaster in June 1972: pp. 71-212.

PALMEIRA, E.M., and MILLIGAN, W.E. 1989. Large scale direct shear tests on reinforced soil. Soils Found. **29**(l): 18-30.

SHEWBRIDGE, S., and SITAR, N. 1985. The influence of fiber properties on the deformation characteristics of fiber-soil composite. Department of Civil Engineering, University of California, Berkeley. Rep. No. UCB/GT/85-02.

TSUKAMOTO, Y. 1987. Evaluation of the effect of tree roots on slope stability. Bull. Exp. For. Tokyo Univ. Agric. Technol. **23** (March): 65-124.

WALDRON, L.J. 1977. The shear resistance of root permeated homogeneous and stratified soil. Soil Sci, Soc. Am. J. **41**(3): 843-849.

WALDRON, L.J., and DAKESSIAN, S. 1981. Soil reinforcement by roots: calculation of increased soil shear resistance from root properties. Soil Sci. **132**(6): 427-435.

Wu, T.H. 1976. Investigation of landslides on Prince of Wales Island, Alaska. Department of Civil Engineering, Ohio State University, Columbus. Geotech. Eng. Rep. No. 5.

ZIEMER, R.R., and SWANSTON, D.N. 1977. Root strength changes after logging in southeast Alaska. USDA For. Serv. Res. Note PNW-306.